

Edge states and topological properties of electrons on the bismuth on silicon surface with giant spin-orbit coupling

D.V. Khomitsky* and A.A. Chubanov

*Department of Physics, University of Nizhny Novgorod,
603950 Gagarin Avenue 23, Nizhny Novgorod, Russian Federation*

We derive a model of localized edge states in the finite width strip for two-dimensional electron gas formed in the hybrid system of bismuth monolayer deposited on the silicon interface and described by the nearly-free electron model with giant spin-orbit splitting. The edge states have the energy dispersion in the bulk energy gap with the Dirac-like linear dependence on the quasimomentum and the spin polarization coupled to the direction of propagation, demonstrating the properties of topological insulator. The electrical conductivity of the edge states is calculated in the presence of finite collision rate and temperature for the varying Fermi level position and is found comparable with the conductance quanta. The topological stability of edge states is confirmed by the calculations of the Z_2 invariant taken from the structure of the Pfaffian for the time reversal operator for the filled bulk bands in the surface Brillouin zone which is shown to have a stable number of zeros with the variations of material parameters. The proposed properties of the edge states may support future advances in experimental and technological applications of this new material in nanoelectronics and spintronics.

PACS numbers: 73.20.At, 75.70.Tj, 85.75.-d

I. INTRODUCTION

During the last decade an increasing attention is given to a new class of structures called topological insulators (TI) with promising characteristics both in fundamental aspects of their physics and possible applications in nanoelectronics, spintronics, and fabrication of new magnetic, optical and information processing devices.^{1–5} The principal features of TI include the presence of time-reversal (TR) invariance in the system where the propagating edge states may exist being localized near the boundary of host material and have the dispersion relation which is linear near the origin of their quasimomentum (Dirac-like structure), corresponding to the energies belonging to the insulating gap of the bulk material. The spin of such states is firmly attached to the direction of propagation along the edge, making them protected against backscattering due to the TR invariance which leads to effective cancelling of two scattered states with opposite possible directions of the spin flip which accompanies such backscattering. The existence of such edge states have been shown in numerous theoretical models of TI, and also in the experiments. The materials included graphene,⁶ HgTe/CdTe quantum wells,^{7–10} bismuth,^{11,12} LiAuSe and KHgSb,¹³ as well as general two-dimensional models of paramagnetic semiconductors,¹⁴ the silicene,^{19,20} the topological modal semimetals.²⁴ Also a lot of studies has been devoted to the general properties of two- and three-dimensional models of TI with certain symmetries,^{15–18,20–23} where four topological invariants have been found in 3D TI instead of the single Z_2 invariant in 2D TI.^{1,2,16}

Recently a general group theoretical analysis has been made for the links between the geometry of the Bravais lattice and the properties of TI.²⁵ It should be mentioned that the symmetry arguments have al-

ways played a significant role in classifying the systems as trivial or topologically protected against external perturbations.^{6,15,25–27} The studies of three-dimensional materials were mostly focused on the Bi₂Se₃, Bi₂Te₃ or Bi₂Te₂Se^{1,2,28–30} where also the edge states were constructed explicitly in several models of the finite-size geometry.^{31,32} It can be seen that although the features of the TI are very general and describe a truly novel state of matter, the number of different materials demonstrating these features is currently quite limited. So, it is of interest to find new materials and compounds where possible manifestations of TI may be present, for both fundamental aspects and applied purposes. It is of interest also to understand which properties of the edge states are common for different systems, and which are special, and how all of them are related to the bulk quantum states in a specific model.

Here we consider a model of edge states and connect their properties to the topological characteristics of the host material for a new candidate for the class of topological insulators: the two-dimensional electron gas (2DEG) in a material with strong spin-orbit coupling (SOC) formed at the interface of the monolayer of bismuth deposited on the silicon. This material is characterized by a giant SOC splitting which was observed experimentally also in a number of metal films or the combined materials of the "metal on semiconductor" type,^{33–38} and recently described theoretically.^{38,39} Its huge spin splitting together with the hexagonal type of the lattice creates a certain potential of manifestation of the TI properties, since the spin-resolved bands may evolve into spin-resolved edge states, and the hexagonal type of the lattice is favorable for the TI to exist.²⁵

The properties of 2DEG at the Bi/Si interface have been studied experimentally with the help of angle-resolved photoemission spectroscopy (ARPES)^{33–38,40–42}

applied also to other materials. It was found that this material represents an example of nowadays widely studied class of materials with large (up to 0.2 . . . 0.4 eV) SOC spin splitting of their energy bands, which can be formed in various compound materials or heterostructures of the "metal on semiconductor" type. It is known for many years that that SOC plays an important role in formation of the TI properties,⁴³ including the localization effects of Rashba SOC combined with electron-electron interaction,⁴⁴ the Dirac-cone surface states in Bi₂Se₃⁴⁵ and Bi₂Te_xSe_{3-x},⁴⁶ PbSb₂Te₄ or Pb₂Bi₂Te₂S₃,⁴⁷ and Bi_{1-x}Sb_x,⁴⁸ the topological phases^{49,50} and quantum spin Hall phase in honeycomb lattice,⁵¹ the ultracold Fermi gases,⁵² the spin Hall effect in graphene,⁵³ and the Kondo insulator effects.^{54,55}

Various materials with strong SOC have been a subject of intensive studies throughout recent years, including the structures of Bi deposited on Si-Ge superlattices,⁵⁶ the Pb on Si structure,³⁶ the trilayer Bi-Ag-Si system,³⁵ the structures with monolayer of Pb atoms covering the Ge surface,⁵⁷ or the Pb on Ge structures.⁵⁸ One can mention also new types of triple bulk compounds with strong SOC like GeBi₂Te₄,⁵⁹ BiTeI or other bismuth tellurohalides,⁶⁰⁻⁶² or recently discussed Bi₁₄Rh₃I₉ material.⁶³

In the present paper we adopt the nearly-free model of two-dimensional bulk states in Bi/Si developed earlier³⁸ and applied in the extended form in our previous paper for the description of spin polarization, charge conductivity and optical properties of this promising material³⁹ for the calculation of 1D the edge states of the electrons on the Bi/Si interface in the finite strip geometry. We obtain both the explicit form of the edge wavefunctions and the edge energy spectrum, calculate their spin polarization and Kubo diagonal charge conductance, and link the possible topological stability of their properties to the Z_2 topological invariant studied by the analysis of the time reversal matrix elements behavior in the Brillouin zone.^{1,2,5,6,15,17} The results of our paper are of interest for expanding the knowledge of new materials with the topologically protected properties where the SOC plays a significant role, making them suitable for further applications in spintronics as stable current-carrying and spin-carrying channels.

The paper is organized as following. In Sec.II we briefly described the nearly free-electron (NFE) model of 2D bulk states at Bi/Si interface, and derive a model for the 1D edge states for the electrons in the finite strip geometry. We calculate their spectrum, wavefunctions, and spin polarization. In Sec.III we apply the finite-temperature and finite collision rate Kubo formula for calculations of the diagonal charge conductance of edge states as a function of the Fermi level position. In Sec.IV we reinforce our findings on the edge state stability by considering the topological band properties of the 2D bulk states in Bi/Si, and find the results supporting the presence of the TI phase. Our conclusions are given in Sec.V.

II. MODEL FOR BULK STATES AND EDGE STATES

A. Bulk states

Our model for the 1D edge states is based on the 2D NFE model for the bulk states of 2DEG formed at the interface of the trimer Bi/Si(111) structure³⁸ developed for the description of the spectrum near the M-point of the BZ, and later extended for the modeling of the electron states in the whole BZ.³⁹ This model was compared with its expansion containing the anisotropic terms in the NFE model as well as with an empirical tight-binding model.³⁸ While the details of band structure and the quality of reproduction of experimental ARPES data on energy bands in Bi/Si vary from model to model, the simple NFE model allows to reconstruct the main properties of spin split bands including the magnitude of splitting, the energy gap, and the spin polarization. It also has a major advantage of a straightforward derivation of the edge states in a finite strip geometry, as we shall see below.

In this model, the Hamiltonian $H = H_0 + V$ is written as a sum of free-electron term H_0 corresponding to Rashba paraboloid centered in the Gamma point of the hexagonal BZ, and the crystal potential energy V with the symmetry of the hexagonal lattice. The parameters of both the H_0 and V are fitted as to provide the best correspondence between the model and the experimentally known structure of the bands near the Fermi level.³⁵⁻³⁸ The corresponding Bloch electron wavefunctions are two-component spinors of the following form:

$$\Psi_{\mathbf{k}}^{bulk}(\mathbf{r}) = \sum_n a_{n\mathbf{k}} \psi_{n\mathbf{k}}^{bulk}(\mathbf{r}) \quad (1)$$

where the Rashba eigenstates $\psi_{n\mathbf{k}} = \psi_{\mathbf{k}+\mathbf{G}_n}$ have the form of free electron states with the quasimomentum is shifted to the certain Gamma point and

$$\psi_{\mathbf{k}}^{bulk} = \frac{e^{i\mathbf{k}\mathbf{r}}}{\sqrt{2}} \begin{pmatrix} 1 \\ \pm e^{i\text{Arg}(k_y - ik_x)} \end{pmatrix}. \quad (2)$$

The (\pm) sign corresponds to two eigenvalues for Rashba energy spectrum $E(k) = \hbar^2 k^2 / 2m \pm \alpha_R k$, and the material parameters are the same as in the previous papers on Bi/Si states,^{38,39} obtained for the best fit to the experimental ARPES data, namely, $m = 0.8m_0$, $\alpha_R = 1.1 \text{ eV} \cdot \text{\AA}$ and $V_0 = 0.3 \text{ eV}$.

In Fig.1 we plot the energy spectrum of 2DEG at the Bi/Si(111) surface in the NFE model.^{38,39} Four lowest bands are shown with the Fermi level position reported experimentally³⁸ to be between the bands 2 and 3 where a gap of around 0.2 eV is formed, creating the possibility of the edge states existence within this gap and making the system a possible new candidate for the topological insulator class. The large metallic-like values of electron energy and SOC amplitude present for the 2DEG

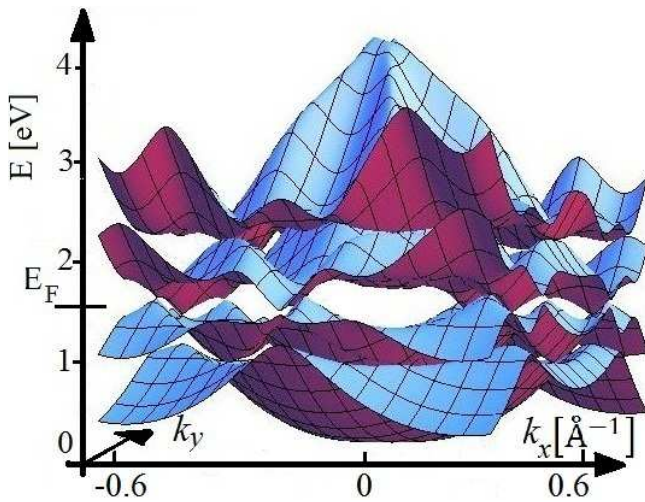


FIG. 1: (Color online) Energy spectrum of 2DEG at the Bi/Si(111) surface in the nearly free-electron model. Four lowest bands are shown with the Fermi level position reported experimentally³⁸ to be between the bands 2 and 3 where a gap is formed creating the possibility of the edge states existence within this gap, and making the system a possible new topological insulator.

in this system make it promising for the consideration in transport and optical experiments where the disorder, collision and thermal broadening prevent the application of conventional semiconductors. It should be noted that the discussed properties of the band structure for Bi/Si 2DEG are obtained in the framework of one specific model with a set of parameters chosen for the best fit to experimental data. Thus, it may be modified in the future when more insight will be gained on the properties of Bi/Si or other similar compounds. Still, we shall see below that the qualitative and topologically described features of the electron states studied within this model are robust against the significant variations of the model parameters, which is an indication of certain intrinsic and stable properties of the system.

B. Edge states

We now turn our attention to the construction of the model for the edge states localized at the opposite edges of the finite strip formed in the 2DEG. We can start with the strip geometry where the electrons are confined along the y direction in the strip $-L/2 \leq y \leq L/2$ and with conventional assumption of the hard-wall boundary conditions $\Psi(x, y = \pm L/2) = 0$.^{8–10,31,32}

First, the spectrum of edge states can be found by solving the eigenstate problem with the requirement of exponential dependence across the strip direction Oy . It can be done by starting from the bulk Hamiltonian and replacing the quasimomentum component in the direction of confinement by the pure imaginary variable de-

scribing the inverse localization depth corresponding to the localized states $\exp(\pm\Lambda y)$ which means in our case the substitution $k_y \rightarrow -i\Lambda$. The eigenfunctions of this Hamiltonian can be constructed in the same nearly free-electron approximation as the bulk states (1), and have the following form:

$$\Phi_{k_x\Lambda}(x, y) = e^{\Lambda y} F_{k_x\Lambda}(x), \quad (3)$$

$$F_{k_x\Lambda}(x) = \sum_n a_n(k_x, \Lambda) \phi_{nk_x\Lambda}(x). \quad (4)$$

The spinors $\phi_{nk_x\Lambda}(x)$ can be obtained from (2) with the substitution $k_y \rightarrow -i\Lambda$,

$$\phi_{nk_x\Lambda}(x) = \frac{e^{i(k_x+nb)x}}{\sqrt{2}} \begin{pmatrix} 1 \\ \pm e^{i\text{Arg}[-(k_x+nb+\Lambda)]} \end{pmatrix}. \quad (5)$$

The summation in (4) is over the 1D lattice in the reciprocal space which corresponds not to 2D hexagonal but the 1D simple lattice along the Ox direction with the period $a = 2\pi/b$ where $b = 1.08 \text{ \AA}^{-1}$ is the reciprocal space period in the k_x direction. The state (4) remain to be Bloch function along Ox with the conventional translational property $\Phi_{k_x\Lambda}(x+a, y) = e^{ik_x a} \Phi_{k_x\Lambda}(x, y)$, while along the confinement direction the wavefunctions are exponents $\exp(\pm\Lambda y)$.

The wavefunction satisfying the boundary conditions on a single edge $\Psi(x, y = \pm L/2) = 0$ and having the specific energy $E = E(k_x, \Lambda)$ in the bulk gap has the form of linear combinations of (4) with different exponents corresponding to the given energy $E = E(k_x, \Lambda)$:

$$\Psi_{k_x}(x, y) = \sum_{\Lambda} c_{\Lambda} \Phi_{k_x\Lambda}(x, y). \quad (6)$$

If we solve the Schrödinger equation for our model of 2DEG at Bi/Si interface and with the substitution $k_y \rightarrow -i\Lambda$, the spectrum of edge states will be obtained as a function of two quantum numbers (k_x, Λ) . If there are eigenstates with energies corresponding to the gap in the bulk spectrum, one can be interested in them as in potential candidates for the edge states with topological protection. We have found that in our model that such energy levels for the edge states indeed exist in the gap of the bulk spectrum, and their dependence on the (k_x, Λ) quantum numbers is shown in Fig.2. The energy depends on two quantum numbers (k_x, Λ) , so the spectrum in Fig.2a is plotted in a 3D layout where the bulk gap edges are shown by two horizontal lines. The existence of two Dirac-like 1D crossing branches of energy (pairs of linear dispersion curves) as functions of k_x is clearly seen at the line $k_x = 0$ of the 1D Brillouin zone, making these edge states promising for being topologically protected. An important feature of the edge state spectrum is the presence of two roots $\Lambda_{1,2}$ for each value of energy for a given k_x , i.e. the equation $E(k_x, \Lambda) = E_0$ has two pairs

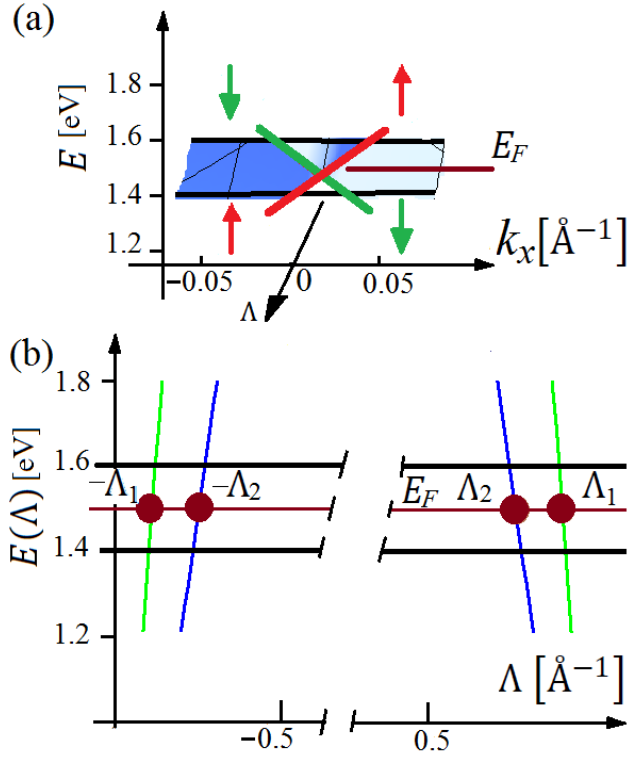


FIG. 2: (Color online) (a) Energy spectrum of edge states located in the bulk energy gap of the Bi/Si(111) surface. The energy depends on two quantum numbers (k_x, Λ) before the boundary conditions are applied. The existence of two Dirac-like 1D crossing branches of energy with the spin polarization S_y connected to the direction of propagation is clearly seen, making these edge states promising for being topologically protected. The spin-up states are moving to the right ($v_x > 0$) while the spin-down states are moving to the left ($v_x < 0$), shown in the same color with corresponding branches of the edge spectrum. (b) Edge state energy dependence on the inverse localization length Λ for the cross-section $k_x = 0.05 \text{ \AA}^{-1}$. For the given position of the Fermi level in the bulk gap there are two roots $\pm\Lambda_{1,2}$ for each edge of the strip giving two edge wavefunctions belonging to the corresponding branches of energy spectrum.

of solutions $\pm\Lambda_{1,2}$ for the left and right edge of the strip, respectively, as it is shown in Fig.2b for the cross-section $k_x = 0.05 \text{ \AA}^{-1}$. Such structure of energy eigenvalues is the direct consequence of the relative proximity of two branches of Rashba spectrum present in the basis for the Hamiltonian which can be also seen for the bulk spectrum in Fig.1. This feature allows one to construct the edge states satisfying the boundary conditions for the band of energies located in the bulk energy gap, as it is done in various models of edge states in TI.^{8,9,31,32} In Fig.2 we also plot the mean values of the only nonvanishing spin component $S_y = \langle \Psi | \sigma_y | \Psi \rangle$ for the edge states which is clearly seen to be connected with their direction of motion along the strip. The spin-up states are moving to the right with the group velocity $v_x = \frac{1}{\hbar} \frac{\partial \varepsilon}{\partial k_x} > 0$ while

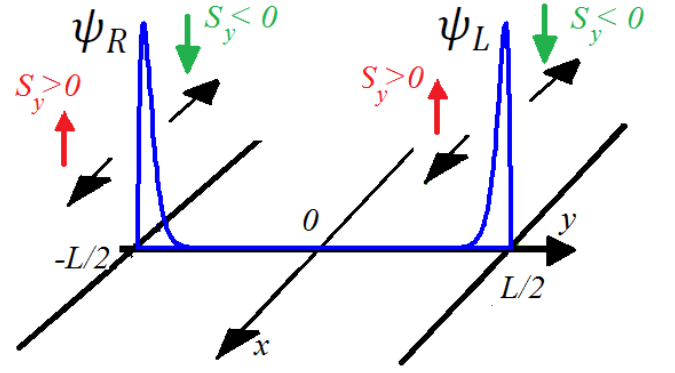


FIG. 3: (Color online) Edge states localized on the opposite borders of the strip (shown schematically) for the energy of the edge state equal to the Fermi level inside the bulk gap $E_F = 1.5 \text{ eV}$ and for the strip width $L = 10 \text{ nm}$. The edge states are well-localized at the corresponding edge of the strip. For each edge there are two states propagating to the positive and negative directions of the Ox axis and having opposite spin polarizations S_y shown nearby the arrow labeling the direction of movement with the color as in Fig.2. The backscattering is possible only with the spin flip, making these states effective for the charge transport along the edge.

the spin-down states are moving to the left ($v_x < 0$), shown in the same color with corresponding branches of the edge spectrum. It is known that this chiral property of edge states makes them topologically protected against backscattering in the TR-invariant system, providing a substantial contribution to the overall conductance in the transport experiments.^{1,2,8}

The specific boundary conditions are applied to the general form of the edge state (6). The two wavefunctions for the given energy $E = E(k_x, \Lambda_{1,2})$ satisfying the boundary condition $\Psi_L(x, y = L/2) = 0$ on the left edge of the strip $y = L/2$ (when facing in the forward direction of the Ox axis) and decaying into the strip, has the form (6) which can be constructed explicitly by the following superposition of the states (4):

$$\Psi_L^{(1)}(x, y) = F_{k_x \Lambda_1}(x) \left(e^{\Lambda_1 y} - e^{(\Lambda_1 - \Lambda_2) \frac{L}{2} + \Lambda_2 y} \right), \quad (7)$$

$$\Psi_L^{(2)}(x, y) = F_{k_x \Lambda_2}(x) \left(e^{\Lambda_2 y} - e^{(\Lambda_2 - \Lambda_1) \frac{L}{2} + \Lambda_1 y} \right) \quad (8)$$

where the normalization condition is implied in $F_{k_x \Lambda}(x)$. Correspondingly, the wavefunction for the right edge $y = -L/2$ can be written as

$$\Psi_R^{(1)}(x, y) = F_{k_x - \Lambda_1}(x) \left(e^{-\Lambda_1 y} - e^{(\Lambda_1 - \Lambda_2) \frac{L}{2} - \Lambda_2 y} \right), \quad (9)$$

$$\Psi_R^{(2)}(x, y) = F_{k_x - \Lambda_2}(x) \left(e^{-\Lambda_2 y} - e^{(\Lambda_2 - \Lambda_1) \frac{L}{2} - \Lambda_1 y} \right) \quad (10)$$

An example of the edge wavefunctions is shown in Fig.3 for the energy of the edge state equal to the Fermi level inside the bulk gap $E = E_F = 1.5$ eV and for the strip width $L = 10$ nm. One can see that the edge states are well-localized at the corresponding edge of the strip on the length of about 1 nm. The arrows indicate the direction of propagation and the spin S_y of each state in pair (7),(8) and (9),(10). The direction of the propagation of two chiral states on the one edge $y = -L/2$ in our model is the same as on the other edge $y = L/2$ which is different from the most of the TI models. This difference can be explained due to the strong Rashba SOC in our system which leads, for example, to the dominant polarization S_y of the states moving in the Ox direction and where the non-compensated total spin S_y can be accumulated if the population of right-moving and left-moving electrons is unbalanced, for example, by external electric field,⁶⁴ which is also can be expected for the edge states shown in Fig.3.

The form of spin polarization shown in Fig.2 creates a positive expectation about their topological stability for the charge transport against the scattering on non-magnetic impurities which do not violate the TR symmetry. If we consider the backscattering, then it is clear from Fig.2 that the change of the propagation direction will lead to the spin flip, and such reversal cancels the reflected waves and extinguishes the backscattering.^{1,2} This is consistent with the arguments of the topological stability of such edge states as the participants of charge transport, which is the required property of a system to become a topological insulator. We shall see below in Sec.IV that our assumption about the 2DEG on the Bi/Si interface as a possible TI is supported further by the analysis of the topological properties of 2D bulk states.

III. CHARGE CONDUCTANCE

An important property of the edge states is their contribution to the total conductance of the sample which was considered in a number of papers on TI.^{9,31,32} It is of interest to consider its dependence on the Fermi level position inside the bulk gap which can be tuned experimentally. Here we perform such calculation for the 1D edge states (6) taking into account the finite collision broadening and considering various temperatures which can be present in future experimental or technological setups with the 2DEG at the Bi/Si interface in a finite strip geometry.

We start with the conventional Kubo formula⁶⁵ for the DC conductance tensor $\sigma_{\mu\nu}$ in a system with volume Ω obtained at finite collision rate $1/\tau$ and with the Fermi temperature function f_i in the i -th band with energy E_i :

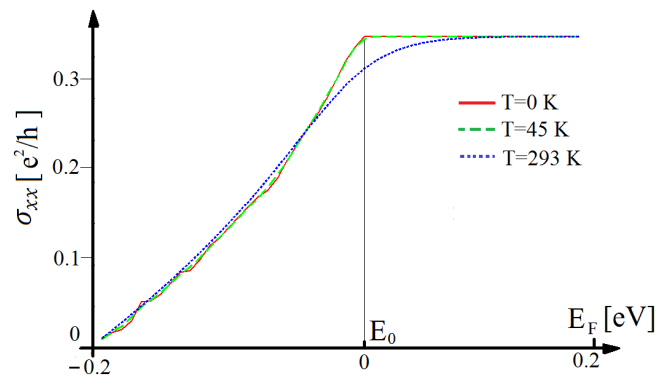


FIG. 4: (Color online) The diagonal charge conductance σ_{xx} is plotted in units of e^2/h as a function of the Fermi level position inside the bulk gap counted from the crossing point of two branches of the edge state dispersion curves for (a) $T = 0$ K (solid curve), (b) $T = 45$ K (dashed curve), and $T = 293$ K (dotted curve). The finite collision rate and finite temperature lead to the maximum values of σ_{xx} significantly below the ballistic value e^2/h . When the Fermi level passes above the crossing point E_0 of the edge state spectrum, new vacant states are no longer available for the electric field-induced transitions, and the conductance saturates. The temperature increase only smooths the conductivity curves due to the large SOC and band gaps in the Bi/Si system being of the order of 0.1 eV which exceeds the scale of thermal energy.

$$\sigma_{\mu\nu} = \frac{2e^2}{\Omega} \sum_{ij} \frac{f_j - f_i}{E_i - E_j} \frac{\hbar^2/\tau}{(E_i - E_j)^2 + (\hbar/\tau)^2} (v_\nu)_{ij} (v_\mu)_{ji}, \quad (11)$$

where $(v_\nu)_{ij}$ are the matrix elements of the velocity operator $v_\nu = \frac{1}{\hbar} \frac{\partial H}{\partial k_\nu}$ which contains the SOC ("anomalous") term due to the presence of Rashba SOC in the Hamiltonian.

The off-diagonal (Hall) conductivity σ_{xy} vanishes since our system is not in a magnetic field, and is internally nonmagnetic. The diagonal charge conductivity σ_{xx} calculated by Eq.(11) is plotted in Fig.4 as a function of the Fermi level position inside the bulk gap counted from the average crossing point $E = E_0$ of two branches of the edge state dispersion curves (see Fig.2). We consider various temperatures $T = 0, 45$ and 293 K, and a realistic value of collision rate $1/\tau = 10^{12} \text{ sec}^{-1}$, although the precise values of scattering parameters in the Bi/Si 2DEG are yet to be determined from the experiments.

One can see in Fig.4 that the conductivity of the edge states even with the inclusion of the collision rate (i.e. in a non-ballistic regime) reaches a significant value in units of conductance quanta e^2/h which makes the edge state in Bi/Si a promising candidate for the charge transport in the bulk insulating regime which has been already reported as being significant in the experiments on TI.^{1,2,8} It should be noted that the maximum of the conductivity in Fig.4 is below the ballistic value e^2/h . The reason is that we consider a non-ballistic regime with finite colli-

sion rate $1/\tau$ and finite temperature, both producing a diminishing effect on the conductivity obtained from the Kubo formula. Such drops of values for the edge state conductivity below e^2/h have been predicted also for the 1D⁹ and 2D³² models of edge state where finite temperatures were taken into account.

The value of σ_{xx} rises when the Fermi level is moving from the lower edge of the bulk gap to the crossing point E_0 for the Dirac-like dispersion, and after passing through this point the conductance saturates. This can be explained by considering the transitions from the lower (occupied) to the upper (vacant) states in the edge spectrum which all contribute to the conductance as long as the interband transitions dominate for the velocity matrix elements in (11). When the Fermi level goes above the crossing point in Fig.2, new vacant states are no longer available for the dominating direct transitions since there is no more empty bands for the edge states is left above the Fermi level, so the total conductance tends to saturate. Since the energy spectrum shown in Fig.2a has a form of Dirac flat cone only along the k_x direction and is described by a essentially different dependence along the Λ direction as it can be seen in Fig.2b, the behavior of conductivity with respect to Fermi level variations is different from the pure Dirac spectra both in 1D and 2D models of TI.^{9,31,32} One can see from Fig.4 that the temperature increase mainly smoothes of the conductivity curve without the major changes in its dependence due to the large SOC and large band gaps in the Bi/Si system of the order of 0.1 eV which exceed the scale of thermal energy even at room temperature, making the Bi/Si a promising candidate for the stable charge transport setups with the help of edge states in future room-temperature devices.

IV. TOPOLOGICAL PROPERTIES OF BULK STATES

It is known from the general theory that the stability of edge states is guaranteed by certain topological properties of the bulk states. In particular, the system can be a TI if an integer called Z_2 invariant is different from zero.^{1,2,6,15} There are several ways for calculation of this invariant, and here we shall use the method proposed by Kane and Mele⁶ which links the Z_2 index to the zeros of the Pfaffian for the interband matrix elements of the time reversal operator which has the form $\Theta = i\sigma_y K$ for the spin-1/2 particles, and K is the complex conjugation operator. If we have only two lowest bands occupied which is the case of our Bi/Si 2DEG (see Fig.1), then the Pfaffian $P_{1,2}(\mathbf{k})$ is equal to the single off-diagonal matrix element between the Bloch functions $u_{1,2}(\mathbf{k})$ in the occupied bands 1 and 2,

$$P_{1,2}(\mathbf{k}) = \langle u_1(\mathbf{k}) | \Theta | u_2(\mathbf{k}) \rangle. \quad (12)$$

The topological considerations provide a convenient

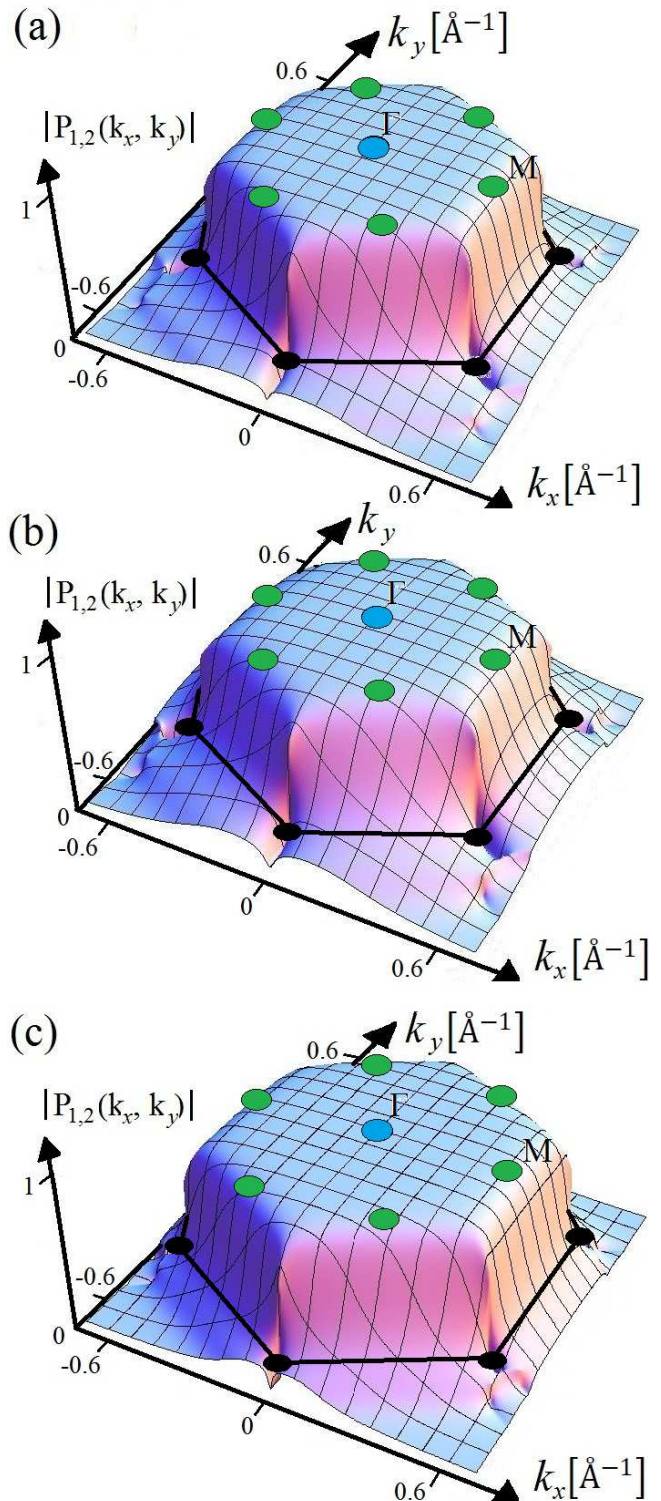


FIG. 5: (Color online) Absolute value of the Pfaffian (12) in the hexagonal BZ for the 2DEG on the Bi/Si interface for different values of bulk band parameters, (a) $V_0 = 0.3$ eV, $\alpha_R = 1.1$ eV \cdot \AA ; (b) $V_0 = 0.6$ eV, $\alpha_R = 1.1$ eV \cdot \AA ; (c) $V_0 = 0.3$ eV, $\alpha_R = 0.6$ eV \cdot \AA . The Pfaffian has three pairs of zeros at the corners of the BZ where the visible zeros are shown as black circles while at TR-invariant Γ and M points shown as blue and green circles the value $|P_{1,2}| = 1$. These properties indicate that the Z_2 invariant is odd, and the topological insulator phase is present.

form of using the definition (12) for the challenging task of finding new material demonstrating the properties of TI. Namely, if for the hexagonal BZ the \mathbf{k} -dependent function $P(\mathbf{k})$ has pairs of zeros in the corners of the BZ (or, depending on the overall symmetry, on the lines inside the BZ), then the system demonstrates the properties of TI.^{6,11,15} There is an extensive discussion of the Z_2 invariant properties related to the TI including another definition of it where the matrix elements of TR operator Θ are calculated between the states with opposite wavevectors \mathbf{k} and $-\mathbf{k}$ and the TI is determined by its properties not in the entire BZ but at discrete set of "time reversal invariant points" like Γ or M points. The detailed discussion and all relevant mathematical connections between different approaches on the calculation of Z_2 invariant can be found in the literature.^{1,2,15,17,27,66-68}

In Fig.5a we plot the absolute value of the Pfaffian (12) in the hexagonal BZ for the 2DEG on the Bi/Si interface for the same basic set of model parameters as were used for calculations of the bulk spectrum in Fig.1. In order to see the possible changes in the Z_2 index with the variation of the system parameters, in Fig.5b,c we plot $|P_{1,2}|$ for two other sets of parameters: in Fig.5b the amplitude of the periodic potential is increased compared to the initial case shown in Fig.1, $V_0 = 0.6$ eV and the amplitude of Rashba SOC is the same, $\alpha_R = 1.1$ eV \cdot \AA . In Fig.5c the periodic potential amplitude is the same as in Fig.5a, $V_0 = 0.3$ eV, but the Rashba coupling amplitude is decreased, $\alpha_R = 0.6$ eV \cdot \AA . It is clearly seen for all cases that the Pfaffian has zeros in the corners of the BZ where the visible zeros are shown as black circles which border is shown schematically, while $|P_{1,2}| = 1$ in the TR-invariant Γ and M points shown as blue and green circles, respectively. There are three pairs of zeros for $|P_{1,2}|$ which indicates that the Z_2 invariant is odd, thus classifying the 2DEG at the Bi/Si interface as a topological insulator with the protected edge states.^{1,2,6,15}

One can see in Fig.5 that the variations of material parameters do not change significantly the topological properties of the Pfaffians which all have the same qualitative features with $|P_{1,2}| = 1$ at the TR-invariant Γ and M points and with three pairs of zeros for $|P_{1,2}|$ in the corners of the BZ. The depth of the parameter variation present in three parts of Fig.5 is rather big and reaches

50% which covers a wide range of possible experimental realization of the 2DEG at the Bi/Si interface. Still, the absolute values of Pfaffians shown in Fig.5 look very similar to each other which indicates their qualitative topological nature being the key for discovering new examples of topological insulators. The method of mutual analysis of chiral edge states and topological bulk properties used in our calculations can be applied to other materials and structures.

V. CONCLUSIONS

We have derived a model for the one-dimensional edge states for the electrons on the bismuth on silicon interface in the finite strip geometry. Based on the bulk nearly free-electron model, their energy dispersion was obtained inside the bulk gap being linear in the quasimomentum. The spin polarization of edge states is linked to the direction of propagation along the given edge which provides topological stability of these chiral modes. The diagonal charge conductance of the edge states was calculated as a function of the Fermi energy for finite collision broadening and finite temperatures, and has shown a specific behavior with respect to the Fermi level position relative to the edge state dispersion curves which may help in their experimental detection. The topological stability of edge states was confirmed by the structure of the interband matrix element for the time reversal operator which was shown to be stable against the large variations of material parameters. The results of the paper may be of interest both for the development of the topological insulator theory by providing a novel example of the material belonging to this class, and also for the development of new spintronics and nanoelectronics devices with stable transport and operating at room temperature.

Acknowledgements

The authors are grateful to V.Ya Demikhovskii, A.M. Satanin, A.P. Protogenov, G.M. Maximova, V.A. Burdov and A.A. Konakov for helpful discussions. The work is supported by the Russian Foundation for Basic Research (Grants No. 13-02-00717a, 13-02-00784a).

* Electronic address: khomitsky@phys.unn.ru

¹ M.Z. Hasan and C.L. Kane, Rev. Mod. Phys. **82**, 3045 (2010).

² X.-L. Qi and S.-C. Zhang, Rev. Mod. Phys. **83**, 1057 (2011).

³ J.E. Moore, Nature **464**, 194 (2010).

⁴ D. Culcer, Physica E **44**, 860 (2012).

⁵ X.-L. Qi, T.L. Hughes, and S.-C. Zhang, Phys. Rev. B **78**, 195424 (2008).

⁶ C.L. Kane and E.J. Mele, Phys. Rev. Lett. **95**, 146802 (2005); **95**, 226801 (2005).

⁷ B.A. Bernevig, T.L. Hughes, and S.-C. Zhang, Science **314**, 1757 (2006).

⁸ M. König, H. Buhmann, L.W. Molenkamp, T.L. Hughes, C.-X. Liu, X.-L. Qi, and S.-C. Zhang, J. Phys. Soc. Jpn **77**, 031007 (2008).

⁹ B. Zhou, H.-Z. Lu, R.-L. Chu, S.-Q. Shen, and Q. Niu, Phys. Rev. Lett. **101**, 246807 (2008).

¹⁰ V. Krueckl and K. Richter, Phys. Rev. Lett. **107**, 086803 (2011).

¹¹ S. Murakami, Phys. Rev. Lett. **97**, 236805 (2006).

¹² T.E. Huber, A. Adeyeye, A. Nikolaeva, L. Konopko, R.C.

- Johnson, and M.J. Graf, *Phys. Rev. B* **83**, 235414 (2011).
- ¹³ H.-J. Zhang, S. Chadov, L. MÜchler, B. Yan, X.-L. Qi, J. Kübler, S.-C. Zhang, and C. Felser, *Phys. Rev. Lett.* **106**, 156402 (2011).
- ¹⁴ X.-L. Qi, Y.-S. Wu, and S.-C. Zhang, *Phys. Rev. B* **74**, 085308 (2006).
- ¹⁵ L. Fu and C.L. Kane, *Phys. Rev. B* **74**, 195312 (2006); *Phys. Rev. B* **76**, 045302 (2007).
- ¹⁶ L. Fu, C.L. Kane, and E.J. Mele, *Phys. Rev. Lett.* **98**, 106803 (2007).
- ¹⁷ T. Fukui and Y. Hatsugai, *Phys. Rev. B* **75**, 121403(R) (2007).
- ¹⁸ L. Fu, *Phys. Rev. Lett.* **106**, 106802 (2011).
- ¹⁹ M. Ezawa, *Phys. Rev. Lett.* **109**, 055502 (2012); *Phys. Rev. B* **86**, 161407 (2012); *Phys. Rev. Lett.* **110**, 026603 (2013); arXiv:1303.1245 (2013).
- ²⁰ N.D. Drummond, V. Zólyomi, and V.I. Fal'ko, *Phys. Rev. B* **85**, 075423 (2012).
- ²¹ J.-M. Hou, W.-X. Zhang, and G.-X. Wang, *Phys. Rev. B* **84**, 075105 (2011).
- ²² M. Levin, F.J. Burnell, M. Koch-Janusz, and A. Stern, *Phys. Rev. B* **84**, 235145 (2011).
- ²³ Y. Li, X. Zhou, and C. Wu, *Phys. Rev. B* **85**, 125122 (2012).
- ²⁴ A.A. Burkov, M.D. Hook, and L. Balents, *Phys. Rev. B* **84**, 235126 (2011).
- ²⁵ R.-J. Slager, A. Meszaros, V. Juričić, and J. Zaanen, *Nat. Physics* **9**, 98 (2013).
- ²⁶ B. Douçot, M.V. Feigel'man, L.B. Ioffe, and A.S. Ioselevich, *Phys. Rev. B* **71**, 024505 (2005).
- ²⁷ A.P. Schnyder, S. Ryu, A. Furusaki, and A.W.W. Ludwig, *Phys. Rev. B* **78**, 195125 (2008).
- ²⁸ D. Hsieh, D. Qian, L. Wray, Y. Xia, Y.S. Hor, R.J. Cava, and M.Z. Hasan, *Nature (London)* **452**, 970 (2008).
- ²⁹ K. Miyamoto, A. Kimura, T. Okuda, H. Miyahara, K. Kuroda, H. Namatame, M. Taniguchi, S.V. Eremeev, T.V. Menshchikova, E.V. Chulkov, K.A. Kokh, and O.E. Tereshchenko, *Phys. Rev. Lett.* **109**, 166802 (2012).
- ³⁰ I.A. Nechaev, R.C. Hatch, M. Bianchi, D. Guan, C. Friedrich, I. Aguilera, J.L. Mi, B.B. Iversen, S. Blügel, Ph. Hofmann, and E.V. Chulkov, *Phys. Rev. B* **87**, 121111 (2013).
- ³¹ J. Linder, T. Yokoyama, and A. Sudbø, *Phys. Rev. B* **80**, 205401 (2009).
- ³² H.-Z. Lu, W.-Y. Shan, W. Yao, Q. Niu, and S.-Q. Shen, *Phys. Rev. B* **81**, 115407 (2010).
- ³³ T. Hirahara, T. Nagao, I. Matsuda, G. Bihlmayer, E.V. Chulkov, Yu.M. Koroteev, P.M. Echenique, M. Saito, and S. Hasegawa, *Phys. Rev. Lett.* **97**, 146803 (2006).
- ³⁴ T. Hirahara, T. Nagao, I. Matsuda, G. Bihlmayer, E.V. Chulkov, Yu.M. Koroteev, and S. Hasegawa, *Phys. Rev. B* **75**, 035422 (2007).
- ³⁵ E. Frantzeskakis, S. Pons, H. Mirhosseini, J. Henk, C.R. Ast, and M. Grioni, *Phys. Rev. Lett.* **101**, 196805 (2008).
- ³⁶ J.H. Dil, F. Meier, J. Lobo-Checa, L. Patthey, G. Bihlmayer, and J. Osterwalder, *Phys. Rev. Lett.* **101**, 266802 (2008).
- ³⁷ I. Gierz, T. Suzuki, E. Frantzeskakis, S. Pons, S. Ostanin, A. Ernst, J. Henk, M. Grioni, K. Kern, and C.R. Ast, *Phys. Rev. Lett.* **103**, 046803 (2009).
- ³⁸ E. Frantzeskakis, S. Pons, and M. Grioni, *Phys. Rev. B* **82**, 085440 (2010).
- ³⁹ D.V. Khomitsky, *JETP* **114**, 738 (2012), doi:10.1134/S1063776112030156.
- ⁴⁰ T. Hirahara, K. Miyamoto, I. Matsuda, T. Kadono, A. Kimura, T. Nagao, G. Bihlmayer, E.V. Chulkov, S. Qiao, K. Shimada, H. Namatame, M. Taniguchi, and S. Hasegawa, *Phys. Rev. B* **76**, 153305 (2007).
- ⁴¹ G. Bian, T. Miller, and T.-C. Chiang, *Phys. Rev. B* **80**, 245407 (2009).
- ⁴² K. Sakamoto, H. Kakuta, K. Sugawara, K. Miyamoto, A. Kimura, T. Kuzumaki, N. Ueno, E. Annese, J. Fujii, A. Kodama, T. Shishidou, H. Namatame, M. Taniguchi, T. Sato, T. Takahashi, and T. Oguchi, *Phys. Rev. Lett.* **103**, 156801 (2009).
- ⁴³ D.N. Sheng and Z.Y. Weng, *Phys. Rev. B* **54**, R11070 (1996).
- ⁴⁴ A. Ström, H. Johannesson, and G.I. Japaridze, *Phys. Rev. Lett.* **104**, 256804 (2010).
- ⁴⁵ S. Basak, H. Lin, L.A. Wray, S.-Y. Xu, L.Fu, M.Z. Hasan, and A. Bansil, *Phys. Rev. B* **84**, 121401(R) (2011).
- ⁴⁶ D. Niesner, Th. Fauster, S.V. Eremeev, T.V. Menshchikova, Yu.M. Koroteev, A.P. Protogenov, E.V. Chulkov, O.E. Tereshchenko, K.A. Kokh, O. Alekperov, A. Nadjafov, and N. Mamedov, *Phys. Rev. B* **86**, 205403 (2012).
- ⁴⁷ S.V. Eremeev, I.V. Silkin, T.V. Menshchikova, A.P. Protogenov, E.V. Chulkov, *JETP Lett.* **96**, 780 (2012).
- ⁴⁸ H.-J. Zhang, C.-X. Liu, X.-L. Qi, X.-Y. Deng, X. Dai, S.-C. Zhang, and Z. Fang, *Phys. Rev. B* **80**, 085307 (2009).
- ⁴⁹ G.-W. Chern, *Phys. Rev. B* **81**, 125134 (2010).
- ⁵⁰ A. Rüegg and G.A. Fiete, *Phys. Rev. Lett.* **108**, 046401 (2012).
- ⁵¹ D. Bercioux, N. Goldman, and D.F. Urban, *Phys. Rev. A* **83**, 023609 (2011).
- ⁵² J.D. Sau, R. Sensarma, S. Powell, I.B. Spielman, and S. Das Sarma, *Phys. Rev. B* **83**, 140510(R) (2011).
- ⁵³ A. Dyrdal and J. Barnaś, *Phys. Rev. B* **86**, 161401 (2012).
- ⁵⁴ M. Dzero, K. Sun, P. Coleman, and V. Galitski, *Phys. Rev. B* **85**, 045130 (2012).
- ⁵⁵ L. Craco and S. Leoni, *Phys. Rev. B* **85**, 195124 (2012).
- ⁵⁶ R.H. Miwa, T.M. Schmidt, and P. Venezuela, *Phys. Rev. B* **72**, 125403 (2005).
- ⁵⁷ K. Yaji, Y. Ohtsubo, S. Hatta, H. Okuyama, K. Miyamoto, T. Okuda, A. Kimura, H. Namatame, M. Taniguchi, and T. Aruga, *Nat. Commun.* **1**:17 doi:10.1038/ncomms1016 (2010).
- ⁵⁸ J. Ibañez-Azpiroz, A. Eiguren, E.Ya. Sherman, and A. Bergara, *Phys. Rev. Lett.* **109**, 156401 (2012).
- ⁵⁹ K. Okamoto, K. Kuroda, H. Miyahara, K. Miyamoto, T. Okuda, Z.S. Aliev, M.B. Babanly, I.R. Amiraslanov, K. Shimada, H. Namatame, M. Taniguchi, E.V. Chulkov, and A. Kimura, *Phys. Rev. B* **86**, 195304 (2012).
- ⁶⁰ K. Ishizaka, M.S. Bahramy, H. Murakawa, M. Sakano, T. Shimojima, T. Sonobe, K. Koizumi, S. Shin, H. Miyahara, A. Kimura, K. Miyamoto, T. Okuda, H. Namatame, M. Taniguchi, R. Arita, N. Nagaosa, K. Kobayashi, Y. Murakami, R. Kumai, Y. Kaneko, Y. Onose, and Y. Yokura, *Nat. Materials* **10**, 521 (2011).
- ⁶¹ V. Gnezdilov, D. Wulferding, P. Lemmens, A. Möller, P. Recher, H. Berger, R. Sankar, and F.C. Chou, arXiv:1303.4333 (2013).
- ⁶² S.V. Eremeev, I.A. Nechaev, Yu.M. Koroteev, P.M. Echenique, and E.V. Chulkov, *Phys. Rev. Lett.* **108**, 246802 (2012); G. Landolt, S.V. Eremeev, Yu.M. Koroteev, B. Slomski, S. Muff, M. Kobayashi, V.N. Strocov, T. Schmitt, Z.S. Aliev, M.B. Babanly, I.R. Amiraslanov, E.V. Chulkov, J. Osterwalder, and J.H. Dil, *Phys. Rev.*

- Lett. **109**, 116403 (2012); S.V. Eremeev, I.A. Nechaev, E.V. Chulkov, JETP Lett. **96**, 437 (2012); I.P. Rusinov, I.A. Nechaev, S.V. Eremeev, C. Friedrich, S. Blügel, and E.V. Chulkov, arXiv:1303.4987 (2013).
- ⁶³ B. Rasche, A. Isaeva, M. Ruck, S. Borisenko, V. Zabolotnyy, B. Büchner, K. Koepf, C. Ortix, M. Richter, and J. van den Brink, Nat. Materials, doi:10.1038/nmat3570 (2013).
- ⁶⁴ P. Kleinert, V.V. Bryksin, O. Bleibaum, Phys. Rev. B **72**, 195311 (2005); D.V. Khomitsky, Phys. Rev. B **79**, 205401 (2009).
- ⁶⁵ Y. Murayama, *Mesoscopic Systems*, Wiley-VCH Verlag, Berlin, 2001.
- ⁶⁶ S. Ryu, C. Mudry, H. Obuse, and A. Furusaki, Phys. Rev. Lett. **99**, 116601 (2007).
- ⁶⁷ R. Roy, Phys. Rev. B **79**, 195321 (2009).
- ⁶⁸ R. Yu, X.L. Qi, A. Bernevig, Z. Fang, and X. Dai, Phys. Rev. B **84**, 075119 (2011).